

Accuracy of purely classical description of TiO₂ nanoparticles

Nicolas Gastellu¹ and Rustam Z. Khaliullin^{1,*}

¹*Department of Chemistry, McGill University, 801 Sherbrooke St. West, Montreal, QC H3A 0B8, Canada*

(Dated: September 3, 2018)

FOR CHEM396 REPORT: We compare the efficiencies of a classical forcefields and DFT when simulating the potential energy surface of amorphous TiO₂ nanoparticles.

INTRODUCTION

Titania (TiO₂) has long been the subject of notable research interest due to its high chemical stability and interesting optical, dielectric, mechanical, and photocatalytic properties^{1–4}. While most works focus on TiO₂ in its most stable and common forms, which are all crystalline, a number of technological uses of this material rely on processing into film or powder form which both tend to be amorphous; further modification of the material is then needed to restore a certain level of crystalline order back to it^{5,6}. Dependence on this last step makes titania significantly more difficult and expensive to use in industrial-scale applications, which has motivated researchers to study amorphous TiO₂ (*a*–TiO₂) in hope of being able to use in it cheaper, less processed forms^{7–9}.

One of the defining traits of amorphous materials is their lack of long-range order, which makes their microstructure extremely hard to study experimentally.

[SOME STUDIES THAT SUCCEEDED = purely experimental; THE BEST ONES = mixed expt + comp-*i*, NEED FOR BETTER COMPUTATIONAL MODELS]

Despite this, several research groups have been able to probe the local atomic structure of *a*–TiO₂ with a certain level of detail using a combination of experimental techniques (e.g. wide-angle X-ray scattering, electron diffraction, X-ray absorption structure spectroscopy) and reverse Monte Carlo simulation^{10,11}.

Main focus = Accuracy

- Accuracy of classical forcefields
- Accuracy of ALMO DFT
- Reference = KS DFT
- System = amorphous titania nanoparticles (mention why this system is physically relevant)

SIMULATION DETAILS

A. Classical MD

All classical MD simulations described in this work were ran in the *NpT* ensemble, using the Matsui-Akaogi (MA) potential to model the interactions between pairs of atoms. The MA potential was originally developed for classical MD simulations of the four main polytypes of crystalline TiO₂¹² to accurately simulate the structural properties of titania’s four main polytypes and the elastic constants of rutile (*r*–TiO₂). It is the most

TABLE I. Parameters used for evaluating the MA potentials.

Element	Z ($ e $)	A (Å)	B (Å)	C (Å ³ kJ ^{1/2} mol ^{−1/2})
Ti	+2.196	1.1823	0.077	22.5
O	-1.098	1.6339	0.117	54.0

widely used potential when classically simulating bulk TiO₂ and has been shown by previous studies^{13–15} to be the most adequate force field for predicting the structure and properties of its liquid and amorphous phases. The MA potential describes the short-range interaction between atoms with a Buckingham potential and their long-range electrostatic interaction using the traditional Coulomb term:

$$V_{ij}(r) = f_0 \cdot (B_i + B_j) \cdot \exp\left(\frac{A_i + A_j - r}{B_i + B_j}\right) - \frac{C_i C_j}{r^6} + \frac{e Z_i Z_j}{4\pi\epsilon_0 r}, \quad (1)$$

where r denotes the distance between the two interacting ions i and j , e is the elementary charge, Z_i is the dimensionless ionic charge of ion i , f_0 is a standard force of 4.184 kJmol^{−1}Å^{−1}, and A_i , B_i , and C_i are parameters corresponding to species i . The numerical values of the constants listed above are given in table I.

The atomic structures of the various *a*–TiO₂ nanoparticles described in this work were obtained in multiple steps. We started by melting rutile (*r*–TiO₂) nanocrystals of 198, 390, 768, and 1842 atoms respectively whose structures were previously optimized at the BLYP/DZVP-GTH level of theory (using a plane wave energy cutoff of 2100 Ry) using classical MD in the *NpT* ensemble with $T = 2000$ K and $p_{\text{ext},0} = 0.0$ Pa. We ran this first round of simulations for 40000 timesteps of $\Delta t = 0.5$ fs. The resulting melt was then cooled in three steps; classical MD simulations using the same potentials, ensemble, and number of steps were ran using $T = 1500$ K, 750 K, and 300 K successively, all with $\Delta t = 2.0$ fs. This process simulated the annealing of the melted nanocrystals into a glass which we then studied using Kohn-Sham DFT.

Seeing as the MA potential was originally elaborated to describe the structural properties of *r*–TiO₂, we also generated a set of conformations of a rutile lattice comprised of 72 atoms in the *NpT* ensemble at $T = 300$ K, using the same potential as described above. Doing so provided us with energy values which we expect to be well correlated with the ones we obtain with DFT methods, thus giving us a reference data set to which we could compare the rest of our results.

B. DFT calculations

Having obtained equilibrated atomic structures for nanoparticles of different sizes, we sampled 101 conformations from the last 40 ps of the last cooling run, at which point all four nanoparticles were in equilibrium with $T = 300$ K thermal bath. We then ran a single-point energy calculation on each conformation using KS DFT at the PBE/DZVP level of theory, using a plane wave cutoff of 2000 Ry. We also ran similar DFT calculations on the different configurations of the reference rutile lattice which we also sampled from the last 40 ps of the MD simulation we mentioned in the last paragraph of the last section.

RESULTS AND DISCUSSION

C. Comparing classical forcefields to KS DFT

For each nanoparticle, we compare the classically evaluated energy of every configuration with the energy obtained through a DFT calculation for that same configuration. We plot our results in figures 1-5. This allows us to gauge the accuracy of MA forcefield; if the classical and quantum mechanical results are well correlated, then the purely classical representation of the forces in the nanoparticles is sufficiently accurate to discriminate between slight variations in a given system's configuration and can therefore be used to simulate this system nanoparticles instead of DFT, which is much more computationally expensive.

Comparing the energies obtained using classical MD and those calculated using DFT reveals that a description of the forces inside an $a - \text{TiO}_2$ nanoparticle using only the two-body MA potential is not precise enough to yield an accurate representation of its potential energy surface (PES) (with respect to its atoms' positions). Indeed, plotting the energies yielded by both calculation methods reveals that DFT calculation methods are much more sensitive to a change in a given nanoparticle's atomic configuration than classical methods.

The system for which this is the most obvious is the 768 atom nanoparticle, for which all classically evaluated energies lie within $\sim 10^{-4}$ Ha of each other, while the energies obtained using quantum mechanical methods vary by $\sim 10^{-1}$ Ha. While this effect is most dramatic for the 768 atom system, every other nanoparticle on which we ran similar calculations exhibit significant clustering of the energies obtained using the MA potential about their mean value, while their DFT energies spread out over a much larger interval.

All four nanoparticles we ran these calculations exhibit weak correlation between the DFT-calculated energy values and the energies obtained using the MA potential. Even more surprisingly we find that the two sets of energy values of the different conformations of the rutile lattice were even less correlated than the ones ob-

tained from the amorphous nanoparticles. Indeed, as can be seen in table C, our simulated rutile lattice yielded the lowest value of ρ of all the systems we studied.

In light of this extremely low correlation, we obviously cannot consider our simulated $r - \text{TiO}_2$ lattice a reference system. However this is not overly problematic, it simply suggests that a purely classical two-body description of atomic interactions in TiO_2 in the amorphous or rutile phase is not sufficiently accurate to keep track of small changes in the system's configuration. Moreover the small RMSE values we get for all systems (except the 768-atom nanoparticle) and the fact that all classically obtained energies for a given system are very close to each other suggest that they are still physically sound at a less precise level of analysis. Indeed, if both sets of energy values for each system varied over intervals of similar sizes and yet remained as uncorrelated as we have observed them to be, then we would be in a position to question the validity of even trying to describe TiO_2 using only the MA potential in the first place. However this is not the case; for every system all energies computed classically differ very little. This is consistent with the fact that the atomic configurations from which such energies are computed were obtained from segments of our MD simulations where the system was already at equilibrium with its environment (i.e. the thermal bath) and thus did not vary greatly either. The contrast between the highly clustered classical values and the much more spread out quantum values could therefore suggest that the quantum description of TiO_2 is much more sensitive to changes in the system's conformational changes while using the MA potential cannot meaningfully register such changes yet still provides an internally consistent and physically viable picture of the system. [Maybe: This interpretation of our results is further corroborated by the higher ρ values in smaller systems.]

D. Comparing ALMO DFT with KS DFT

Having observed that DFT calculations are necessary to properly sample from an $a - \text{TiO}_2$ nanoparticle's PES, we are now faced with the problem posed by the computing power necessary to run such calculations on large systems (i.e. nanoparticles containing more than ~ 1000 atoms). Seeing as computational expense is one of DFT's main drawbacks, a number of optimisation schemes have been proposed over the years to reduce both the amount of memory and the time necessary to run such calculations. Among them, we focus our attention to the absolutely localised molecular orbitals (ALMO) method which partitions the system being simulated into smaller fragments (usually these are the individual atoms or molecules that compose it) and runs traditional DFT on each fragment in parallel. This has the advantage of having a runtime that scales linearly with the number of fragments for large systems. Seeing as ALMO DFT makes a number of large DFT calculations much more

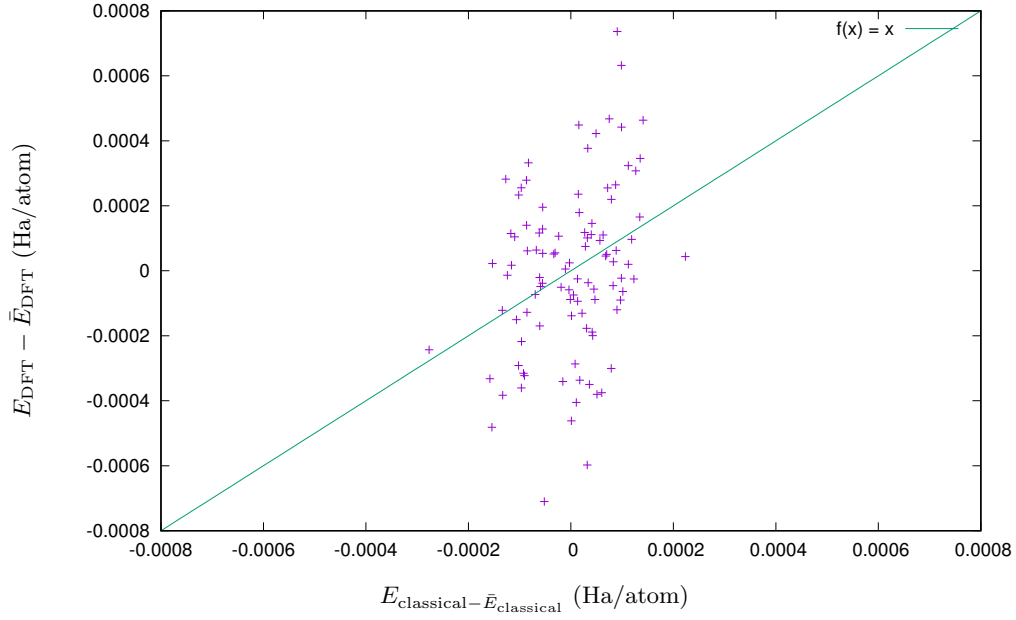


FIG. 1. DFT energy vs. classical energy (both shifted down by their average value) for 101 conformations of an a - TiO₂ nanoparticle with 198 atoms.

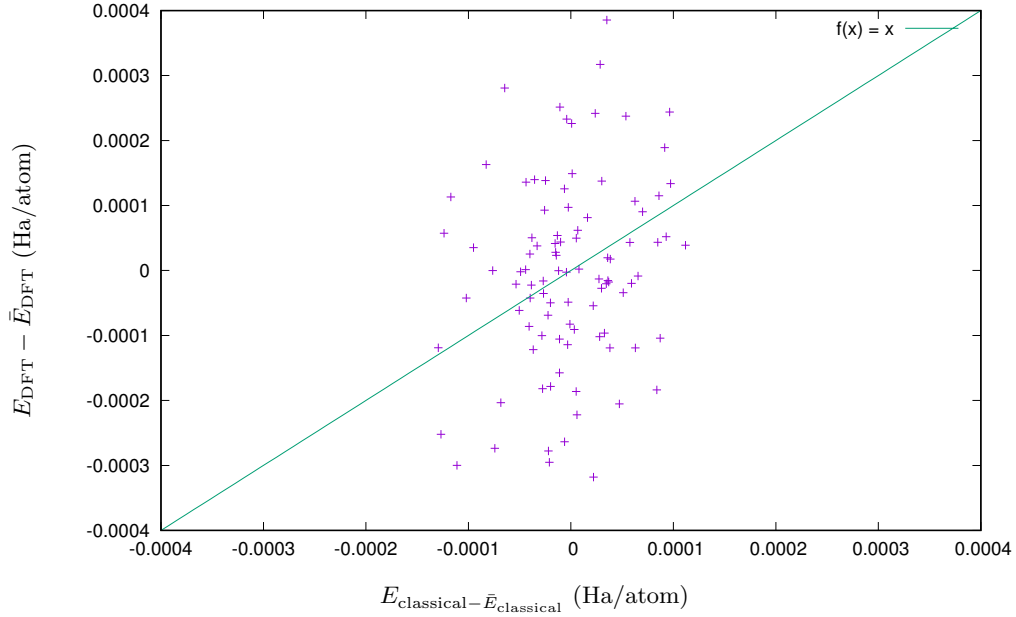


FIG. 2. DFT energy vs. classical energy (both shifted down by their average value) for 101 conformations of an a - TiO₂ nanoparticle with 390 atoms.

feasible, we decide to test its accuracy on our various a - TiO₂ nanoparticles. As before, we evaluate the accuracy of the ALMO DFT method by comparing the energy it outputs for a given configuration of a nanoparticle with the energy obtained through classical DFT.

CONCLUSIONS

- ALMO needed to study size-dependence of certain properties

Acknowledgments. The research was funded by the Natural Sciences and Engineering Research Council of Canada through the Discovery Grant. The authors are

System	$a - \text{TiO}_2$ (198 atoms)	$a - \text{TiO}_2$ (390 atoms)	$a - \text{TiO}_2$ (768 atoms)	$a - \text{TiO}_2$ (1842 atoms)	$r - \text{TiO}_2$ (72 atoms)
ρ	0.3066474	0.3497706	-0.0496755	TBC	0.0141203
RMSE	0.0486056	0.0628487	22.21090	TBC	0.0518275

TABLE II. Pearson correlation coefficient ρ and RMSE between the energy values obtained through DFT and those obtained using the two-body MA potential on various configurations of different systems.

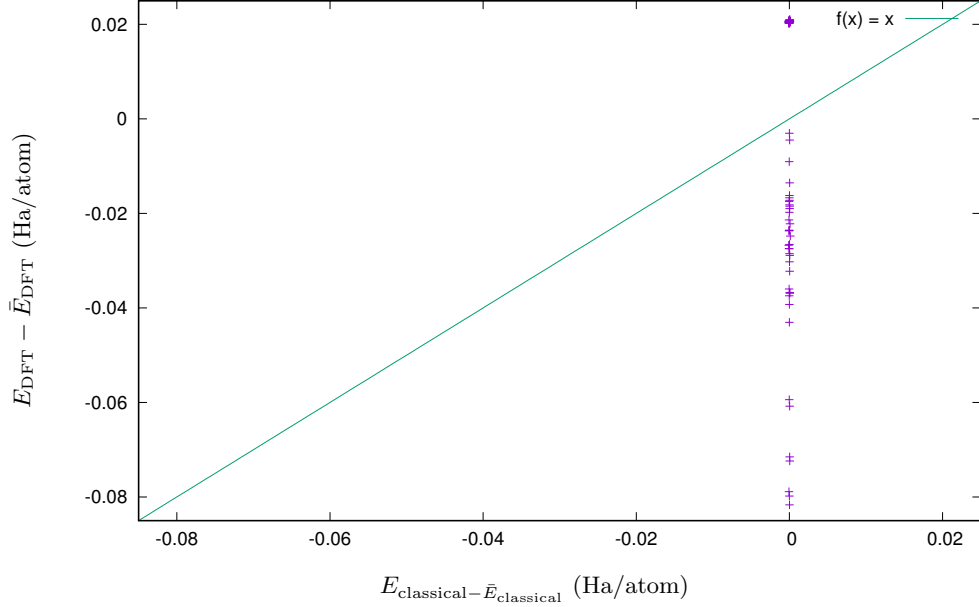


FIG. 3. DFT energy vs. classical energy (both shifted down by their average value) for 101 conformations of an $a - \text{TiO}_2$ nanoparticle with 768 atoms.

grateful to Compute Canada and McGill HPC Centre for computer time.

* rustam.khaliullin@mcgill.ca

¹ P. A. Christensen, A. Dilks, T. A. Egerton, and J. Temperley, “Infrared spectroscopic evaluation of the photodegradation of paint part ii: The effect of uv intensity & wavelength on the degradation of acrylic films pigmented with titanium dioxide,” *Journal of Materials Science* **35**, 5353–5358 (2000).

² K.A. Vorotilov, E.V. Orlova, and V.I. Petrovsky, “Sol-gel tio2 films on silicon substrates,” *Thin Solid Films* **207**, 180–184 (1992).

³ AJ Perry and HK Pulker, “Hardness, adhesion and abrasion resistance of tio2 films on glass,” *Thin Solid Films* **124**, 323–333 (1985).

⁴ Yi Ma, Xiuli Wang, Yushuai Jia, Xiaobo Chen, Hongxian Han, and Can Li, “Titanium dioxide-based nanomaterials for photocatalytic fuel generations,” *Chemical reviews* **114**, 9987–10043 (2014).

⁵ Hengbo Yin, Yuji Wada, Takayuki Kitamura, Shingo Kambe, Sadao Murasawa, Hiroto Mori, Takao Sakata, and Shozo Yanagida, “Hydrothermal synthesis of nano-sized anatase and rutile tio2 using amorphous phase tio2,” *Journal of Materials Chemistry* **11**, 1694–1703 (2001).

⁶ Binay Prasai, Bin Cai, M. Kylee Underwood, James P.

Lewis, and D. A. Drabold, “Properties of amorphous and crystalline titanium dioxide from first principles,” *Journal of Materials Science* **47**, 7515–7521 (2012).

⁷ Jian Zou, Jiacheng Gao, and Fengyu Xie, “An amorphous tio2 sol sensitized with h2o2 with the enhancement of photocatalytic activity,” *Journal of Alloys and Compounds* **497**, 420–427 (2010).

⁸ Miki Kanna, Sumpun Wongnawa, Supat Buddee, Ketsarin Dilokkhunakul, and Peerathat Pinpithak, “Amorphous titanium dioxide: a recyclable dye remover for water treatment,” *Journal of sol-gel science and technology* **53**, 162–170 (2010).

⁹ Hu Young Jeong, Jeong Yong Lee, and Sung-Yool Choi, “Interface-engineered amorphous tio2-based resistive memory devices,” *Advanced Functional Materials* **20**, 3912–3917 (2010).

¹⁰ V Petkov, G Holzhüter, U Tröge, Th Gerber, and B Himmel, “Atomic-scale structure of amorphous tio2 by electron, x-ray diffraction and reverse monte carlo simulations,” *Journal of non-crystalline solids* **231**, 17–30 (1998).

¹¹ Hengzhong Zhang, Bin Chen, Jillian F Banfield, and Glenn A Waychunas, “Atomic structure of nanometer-sized amorphous tio 2,” *Physical Review B* **78**, 214106

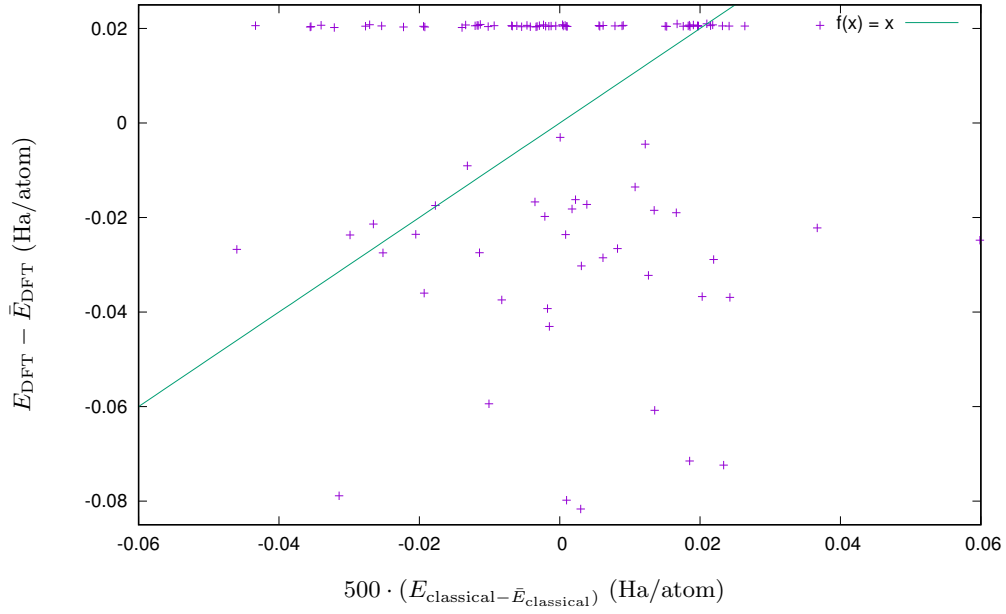
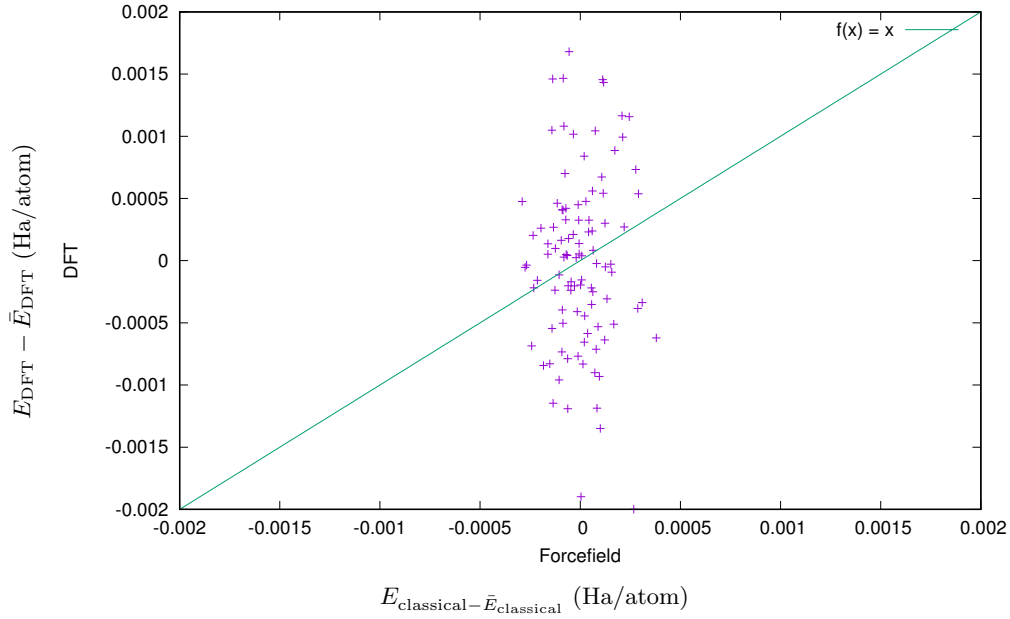


FIG. 4. Rescaled version of figure 3.

FIG. 5. DFT energy vs. classical energy (both shifted down by their average value) for 101 conformations of an r - TiO_2 lattice with 72 atoms.

- (2008).
- ¹² Masanori Matsui and Masaki Akaogi, “Molecular dynamics simulation of the structural and physical properties of the four polymorphs of tio_2 ,” *Molecular Simulation* **6**, 239–244 (1991).
- ¹³ DR Collins and W Smith, *Daresbury Research Report DL-TR-96-001: Evaluation of TiO_2 forcefields.*, Tech. Rep. (Council for the Central Laboratory of Research Councils, 1996).

- ¹⁴ Mozghan Alimohammadi and Kristen A Fichthorn, “Molecular dynamics simulation of the aggregation of titanium dioxide nanocrystals: preferential alignment,” *Nano letters* **9**, 4198–4203 (2009).
- ¹⁵ Vo Van Hoang, “Structural properties of simulated liquid and amorphous tio_2 ,” *physica status solidi (b)* **244**, 1280–1287 (2007).